Light Metals 2015
Edited by: Margaret Hyland
TMS (The Minerals, Metals & Materials Society), 2015

BUBBLE FLOW IN A STATIC MAGNETIC FIELD

Subrat Das[1], Lanka Dinushke Weerasiri, Veeriah Jegatheesan
[1]Deakin University, School of Engineering, 75 Pigdons Road, Waurn Ponds, VIC 3216, Australia

Keywords: Dimensional Analysis, Magneto-hydrodynamics, Hall-Héroult cell

Abstract

A lab-based electrolytic-cell is designed to analyze the effect of external magnetic field on bubble evolution underneath an anode surface. Buckingham Pi theorem is used to provide a complete list of dimensionless parameters for a typical cell configuration.

There is an increase in bubble size and the number of bubbles with time. The hydrodynamic convection is apparent due to the effect of electrolyte flow caused by swarm of bubbles rising along the anode surface. The image sequence shows that swarm of bubbles exhibit a swirling flow-field in the presence of the magnetic field. The coalescence process intensifies in an area where magnetic field is higher. As a consequence, bubbles are swept away by the magneto-hydrodynamic (MHD) convection. These results suggest that a magnetic field causes remarkable improvement on the surface coverage of the anode.

Introduction

Bubble evolution on an electrode surface is governed by electrochemical reactions and is a challenging topic in many electrolysis processes [1]. It is assumed that the gas produced in molecular form is transformed to the gaseous state and subsequently nucleate in the form of bubbles. The internal pressure of the bubble (also known as Laplace pressure) is always more than the hydrostatic pressure of surrounding fluid (electrolyte) and plays an important role in understanding bubble-surface interaction. There are many industrial applications such as submerge gas injection, drug delivery, vapor nucleation on a submerged hot plate, mass transport in fluidized bed and gas evolving electrodes, where the influence of the system parameters control the characteristics of bubble flow. The Hall-Héroult cell is a typical example, where bubbles are nucleated underneath a downward facing anode under the influence of an external magnetic field. These gas bubbles have a complex effect on the electrolysis process due to the presence of several forces such as gravity, surface tension, inertia and particularly the magneto-hydrodynamic force (MHD) in the Hall-Héroult cell.

A number of studies on bubble induced flow in an aluminum cell that are carried out in past decades have used physical analogue models (bench-scale) of electrolytic cells [2-6] since experiments on an operating cell are impracticable. Maxworthy [7], reported the influence of various surface forces on bubble rise under an inclined plate submerged in a liquid through his experimental and theoretical techniques. Perron et al. [8] reported the behavior of single air bubble under a downward facing inclined solid surface. Chen et al. [9] studied the effect of various inclination angles. Caboussat [10] reported the morphology of the large bubbles and its influence on the induced velocity field. Most of these experimental data describe the bubble shape, terminal velocity and the bulk electrolyte flow using Reynolds (*Re*), Eötvos (*Eo*), Morton (*Mo*) and Froude (*Fr*) numbers [7, 11, 12]. However, it is important to note that, in the laboratory-based models, the gas bubbles are generated either by nozzle or forcing air through a porous plate, which is in contrast to the Hall-Héroult process, where the bubbles are generated electrolytically in a strong external magnetic field.

On the other hand, electrolytically generated bubbles in aqueous media have gained renewed interest on the study of bubble characteristics. Qian et. al. [13, 14] studied the bubble layer-resistance using aqueous electrolyte. Alam et. al. [15] reported the impact of anode inclination angle on sliding bubbles underneath the anode surface. Despite the efforts made towards the development of lab-based electrolytic cell-models, there still remain several concerns regarding the impact of magnetic field on these bubbles. The dimensionless parameters, discussed above, often used to scale up/down experimental data do not even include the influence of MHD forces. These issues provide the motivation to study the effect of magnetic field on gas-liquid interaction in the electrolysis process.

Dimensional Analysis

Studies of the flow in an electrolytic cell under the influence of an external magnetic-field, have largely been concentrated on motion set up by magnetic forces. The origin of these effects is in Lorentz-force-driven convection. An electrically insulating gas bubble does not experience a direct impact of the Lorentz force, however, the pressure, viscosity, density, surface tension and gravity field of the surrounding conducting fluid are strongly affected by the external magnetic field. In order to give an insight, the MHD interaction parameter is derived from basic dimensional principle. In general, for a two-phase flow system under an isothermal conditions, the bubble velocity for a magnetic induced flow can be expressed as:

$$v_b = f(\rho, \rho_b, \mu, L, d_b, \gamma, g, B, \sigma, Q, V,) \quad (1)$$

where, γ is the surface tension of the continuous liquid phase(electrolyte); μ and ρ are the dynamic viscosity and the density of the electrolyte respectively; ρ_b is the density of gas phase (bubble); v_b is the velocity of bubble, V is the bulk velocity of the electrolyte; g, B and σ are gravity, magnetic field and electrical conductivity respectively; Q is the gas formation rate [2]; $d_b$is the bubble diameter and L is the characteristic length of anode.

We note that the function *f*, in equation 1, involves 12 dimensionally homogeneous variables (i), and four reference variables(j), namely [M]: mass, [L]: length, [T]: time and [A]: Ampere. The Buckingham Pi (π) theorem [16] then dictates that the number of independent dimensionless parameters needed to fully describe the behavior of this system is $i - j$ = 12 - 4 = 8.

Several variables are selectively recurrent in all π terms. In effect, the number of repeating variables equals the number of the reference variables. In the present analysis ρ_b, μ, B and d_b are chosen as repeating variables to create π terms by combining with remaining variables. For example, the first dimensional product with surface tension can be expressed as:

$$\pi_1 = \rho^k, \mu^l, B^m, d_b^n, \gamma \tag{2}$$

The exponents k, l, m and n are obtained from the requirement that π_1 is dimensionless, which leads to the first dimensionless parameter as:

$$\pi_1 = \frac{\rho d_b \gamma}{\mu^2} \tag{3}$$

A similar procedure gives rise to a set of dimensionless parameters, which can be expressed as:

$$\frac{\rho v_b d_b}{\mu} = f\left(\frac{\rho}{\rho_b}, \frac{D}{d_b}, \frac{\rho d_b \gamma}{\mu^2}, \frac{\rho^2 d_b^3 g}{\mu^2}, \frac{\sigma B^2 d_b^2}{\mu}, \frac{\rho Q}{\mu d_b}, \frac{\rho V d_b}{\mu}\right) \tag{4}$$

The most important non-dimensional parameters describing the influence of magnetic field are the Hartmann number and the magnetic interaction parameter (Stuart number), which can be written as[17]:

$$Ha^2 = \frac{\sigma B^2 d_b^2}{\mu} = \frac{Lorentz\ Force}{Viscous\ Shear\ Force}$$

$$N = \frac{\sigma B^2 L}{\rho V} = \frac{Ha^2}{Re} = \frac{Lorentz\ Force}{Inertia\ Force}$$

Experimental Setup

In the aluminum electrolysis process, it is well known that the current traverses in an inclined manner in the molten aluminum [18] due to high electrical conductivity of metal. The inclined current-path is the main source of MHD force in molten aluminum. However, it is impossible to achieve a similar current distribution in a geometrically scaled-down model using aqueous electrolyte. For a parallel arrangement of electrode, current traverses in a vertical direction due to the poor conductivity of electrolyte. Thus, the experimental apparatus designed here aims to achieve some sort of inclined current path in the electrolyte (dynamic similarity) rather than keeping the design geometrically similar to the actual Hall-Héroult cell. Although, we all know that the basis of dimensional analysis (similitude) requires the lab-scale model (scaled down) to be geometrically similar, different systems can have similar characteristics within the framework of dimensional considerations [16].

A schematic of the cold modelling apparatus is illustrated in Figure 1. Aqueous copper sulphate as electrolyte as well as stainless-steel and copper as anode and cathode respectively are used in this model. The choice of electrodes ensures no bubble generation at the cathode end [15]. The apparatus consists of a rectangular tank (300 x 150 mm) of 173 mm high made out of Perspex. The setup inside the vessel comprised an anode holder, steel anode, copper cathode and an insulating partition wall. The anode-holder-block is machined to hold the anode at different inclination angles. The copper cathode is embedded onto the bottom sidewall of the cell to create a current path in an inclined fashion. An insulating barrier with a rectangular slit (as shown in Figure 1) is also placed in between the cathode-sidewall and anode to restrict the interference between copper deposits at cathode with the bulk electrolyte. The electrodes are prepared using fine-grain sandpaper and rinsed with sulphuric acid and distilled water. The anode is insulated all around except the bottom surface, which allows the bubble formation only on the downward facing anode. Aqueous copper sulphate ($CuSO_4$) solutions of 0.5 molar concentration was made up using anhydrous $CuSO_4$ in distilled water and used in all cases. The volume of electrolyte and molar concentration of aqueous $CuSO_4$ and the surface area of anode are calculated to inject 3 A of current into electrolyte using a DC power source, which corresponds to an average current density of 800 A/m^2. It is to be noted that the current density can be increased by changing the electrode surface areas. The sulphate and hydroxide ions release their electrons to the anode and the overall electrolytic reaction is:

$$CuSO_4(aq) + 2e^- + H_2O \rightarrow Cu(s) + H_2SO_4(aq) + {}^1/_2\, O_2(g) \tag{5}$$

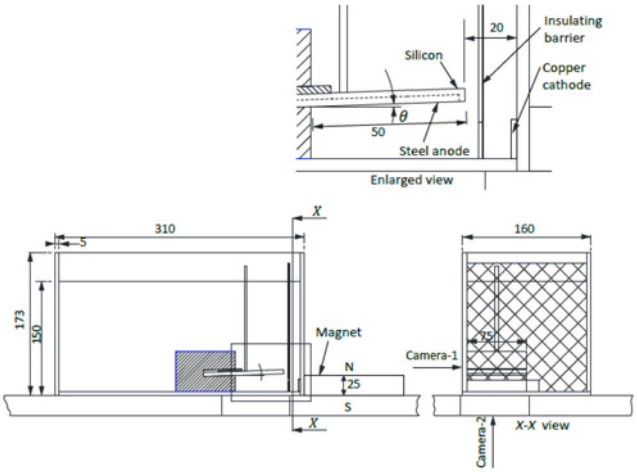

Figure 1. Experimental setup (all dimensions are in mm)

A neodymium-based magnet with surface field of 1.8 T (Tesla) is used as a static external field as shown in figure 1. We know that the magnetic field decays rapidly (exponentially) with distance from the magnet. Magnetic field strength is measured using a gauss meter which varies from 0.1 T (at the far end of the anode) to 0.72 T (approximately) at the sidewall (as shown in Figure 2).

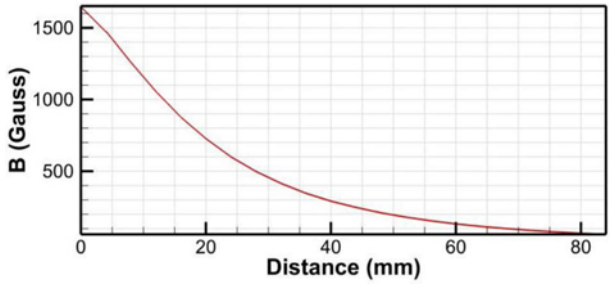

Figure 2 Magnetic field measurement using Gauss meter

A Phantom V711 high speed camera (Camera 1) and Nikon (D7000) digital camera (Camera 2) are used to capture the images of bubble formation. Both cameras are used simultaneously with

the help of trigertrap device to record the direct lateral and the bottom views of anode surface. We made use of a Nikon (DSLR) camera, not so much for its high acquisition frequency but for its capability of producing high quality images. In order to maximise contrast (aqueous copper sulphate not being transparent) a light source is placed at a great distance behind the anode for the lateral view (for high speed camera). A glass diffuser is also used in order to obtain an even light sheet so that the camera can acquire the shadow image of the moving bubbles. Experiments are carried out at different inclination angles of anode ($\theta = 0, 1 \text{ and } 2$ deg) with and without the magnetic field. Image J is used [19] to measure the bubbles sliding velocities and their sliding-paths are plotted using manual tracking based on maximum pixel intensity.

Results and Discussion

The gas bubbles instantaneously nucleate within 0.05 s after the electrolysis has started. The nucleation begins at the anode edge (near to the sidewall) where the maximum current density is expected, as current traverses in a least resistance path. Figure 3 shows the bubble formation at 10 second intervals ($\Delta t = 10s$) on the horizontal anode surface ($\theta \approx 0^o$) without any external magnetic field. There is an increase in bubble size and the number of bubbles with time, which is mainly due to the enhancement of current density due to increased bubble-coverage-area. At higher current densities, the concentration of the dissolved gas at the electrode-electrolyte interface increases that again results in activating more nucleation sites. Alam et. al.[15] also reported similar size of bubbles underneath the anode surface using copper sulphate electrolyte.

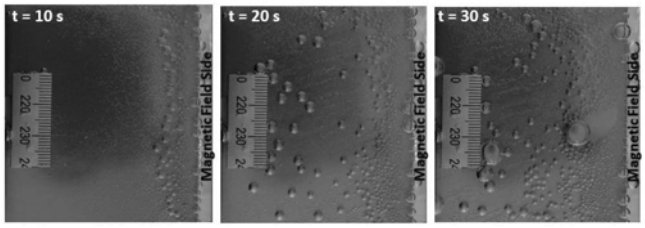

Figure 3 Bubbles under a horizontal anode, $\theta \approx 0, \text{and } B = 0$

Figure 4 (a & b) shows the bubble motion underneath the inclined anodes ($\theta \approx 1 \text{ \& } 2$ deg), without any magnetic field. The electrolyte flow is mostly caused by swarm of bubbles rising on the surface. Smaller bubbles progressively join to form large ones due to coalescence process (Laplace pressure difference). It is clear from the images that larger bubbles usually drift away from the nucleating sites and slide, i.e. when the buoyancy force overcomes the interfacial force, along the anode surface. This would promote the other localised phenomena such as the wake by the surrounding fluid (i.e. the electrolyte) and/or more nucleating sites for bubble to grow. More nucleation always refers to more mass transfer in electrochemical process. However, it is observed that smaller bubbles, when in cluster (or in bubble swarm), exhibit a sluggish flow at some part of anode surface.

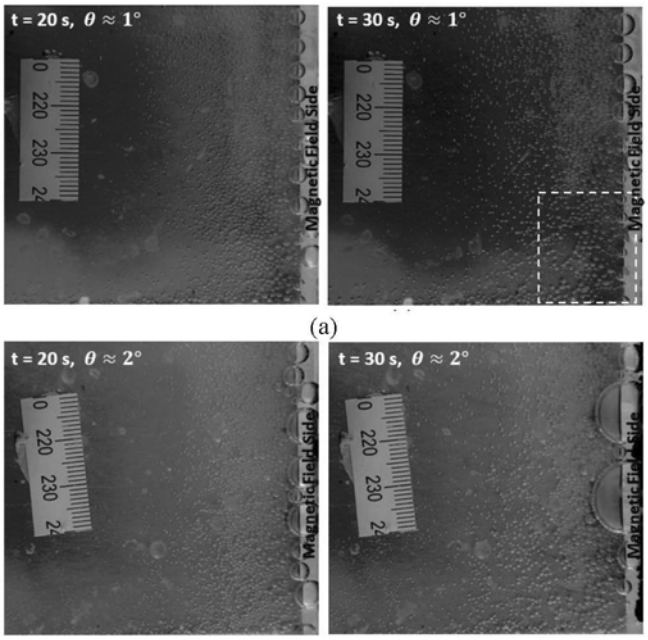

(a)

(b)

Figure 4 Bubble motion underneath the inclined anodes without magnetic field $B = 0$ T

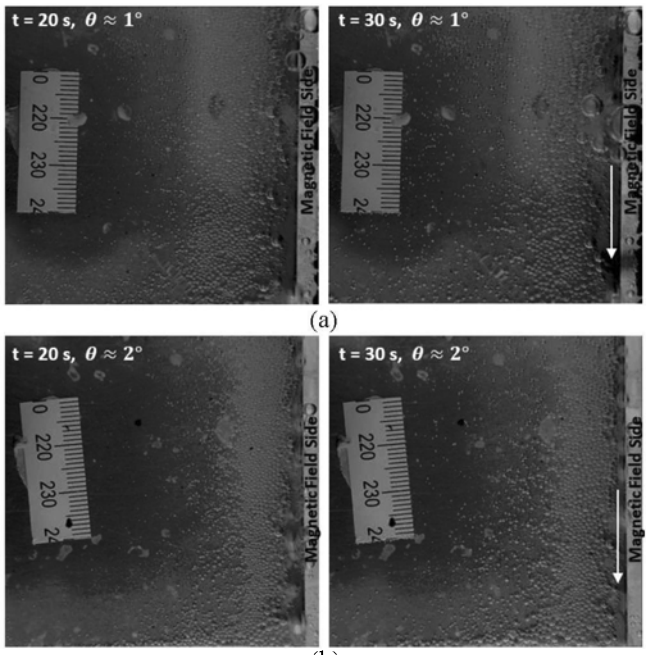

(a)

(b)

Figure 5 Bubble motion underneath the inclined anodes with magnetic field

Figure 5 (a & b) shows the influence of external magnetic field on swarm of bubbles. The onset of MHD convection can be seen (from the bubble motion) in all parts of anode surface since the start of the electrolysis. Higher velocity is observed in all parts of anode surface. The bubbles near the sidewall, i.e. near the edge of anode (as marked by arrow in Figure 5) have maximum velocity at 0.6 T magnetic field but could not be captured by the Nikon DSLR camera. It can be seen that the direction of the bubble/electrolyte flow remains perpendicular to anode inclination

as the MHD forces act orthogonal to both the current and magnetic fields. This finding is of particular interest since the bubble paths observed for very strong magnetic field differ substantially from those of hydrodynamic flows. The electrolyte sweeps all the gas bubbles away from the anode surface (near the edge), thereby impending the bubble coverage growth in the outer part of the anode.

In general, the average bubble-bubble distance becomes shorter with increasing nucleating sites. It is rare to see any single bubble sliding across the anode at small inclination angle ($\theta \leq 2°$). Thus, the behaviour of a bubble largely depends on the characteristics of bubble swarm and consequently the bubble-bubble interaction.

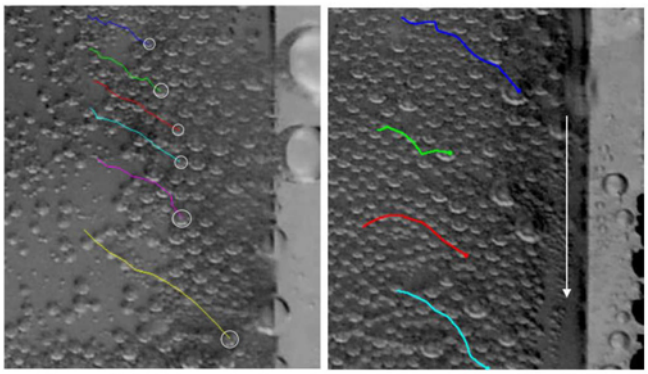

Figure 6 Bubble paths from image sequence (t = 16 s -27 s)

Figure 6 shows the bubble-paths at one corner of the anode surface (see Fig. 4) for a few arbitrarily selected bubbles, from the image -sequence. It is to be noted that the lighting of the front of the anode makes it difficult to observe the growth of any particular bubble. The bubble-paths have been tracked by means of contrast measurement based on a maximum intensity technique. It is clear from Figure 6 that the swarm of bubbles tends to form a rotational path due to the combined effect of buoyancy and MHD fields.

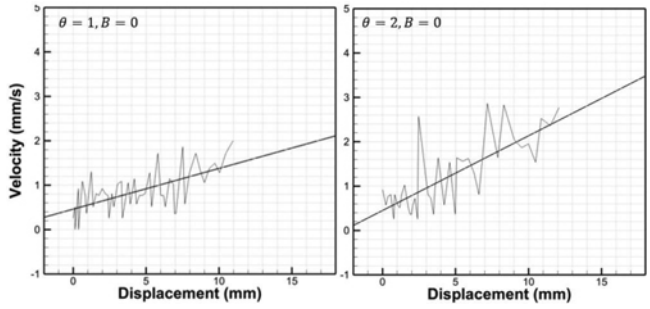

(a)

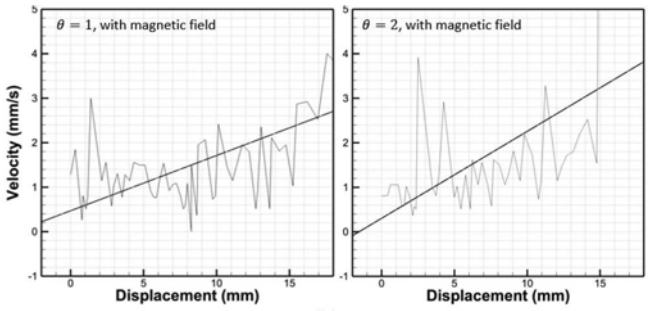

(b)

Figure 7 Velocity of a single bubble

In order to quantify our observations, velocity and distance traversed by a single bubble are calculated from the image sequence and plotted in Figure 7. Obviously, the figure shows a complex velocity pattern due to the coalescence process arising from bubble-bubble interaction. The coalescence of bubbles continuously changes the local pressure field by inducing additional convective forces, showing sharp change in local velocity. As a consequence, larger bubbles remove the smaller bubbles in the vicinity. The solid lines in the figure are straight-line fits of experimental data, which show the increase in velocity with distance and the inclination angle. Figure 7 (b) clearly shows an intensive coalescence process when applied to an external magnetic field. The increase in velocity and the path-traversed indicate the influence of magnetic interaction parameter (N). This strongly suggests that the coalescence process caused by MHD convection is the main source of current enhancement.

Conclusion

The lab-based-cell is designed to achieve a dynamic similarity between the model and Hall-Héroult cell to study the impact of MHD convection.

The primary forces found to be governing overall bubble behaviour are the inertial forces derived from the flow and the buoyancy force of the bubble without the presence MHD forces.

It has been clearly demonstrated that the superposition of a magnetic field during aqueous $CuSO_4$ electrolysis, regardless of its orientation (anode inclinations), significantly affects the bubble density, coalescence, velocity and the overall sliding characteristics. The enhancement of the coalescence process and the bubble velocity in the presence of a magnetic field is surprising, since it implies the dominance of MHD induced flow rather than simply a 'bubble induced flow', as was previously thought. In future, we are planning to use Particle Image Velocimetry (PIV) to quantify the velocity field to relate the magnetic interaction parameter to swarm of bubbles.

References

1. H. Matsushima, T. Iida, and Y. Fukunaka, "Gas bubble evolution on transparent electrode during water electrolysis in a magnetic field," *Electrochimica Acta*, 100 (2013), 261-264.
2. A. Solheim et al., "Gas induced bath circulation in aluminium reduction cells," *Journal of Applied Electrochemistry*, 19 (5) (1989), 703-712.
3. A. Solheim and J. Thonstad, "Model Cell Studies of Gas

Induced Resistance in Hall--Heroult Cells," *Light Metals*, 2 (1986), 397-403.
4. L.I Kiss, "Transport Processes and Bubble Driven Flow in the HALL-HÉROULT Cell," *Fifth International Conference on CFD in the Process Industries*, (2006).
5. G.Q. Yang et al., "Bubble formation and dynamics in gas–liquid–solid fluidization—A review," *Chemical Engineering Science*, 62 (1-2) (2007), 2-27.
6. M.A. Cooksey et al., "Effect of slot height and width on liquid flow in physical models of aluminium reduction cells," *Light Metals*, 2 (2007), 451-456.
7. T. Maxworthy, "Experimental studies in magneto-fluid dynamics: pressure distribution measurements around a sphere," *Journal of Fluid Mechanics*, 31 (4) (1968), 801-814.
8. A. Perron et al., "An experimental investigation of the motion of single bubbles under a slightly inclined surface," *International Journal of Multiphase Flow*, 32 (5) (2006), 606-622.
9. J.J.J. Chen et al., "Resistance due to the presence of bubbles in an electrolytic cell with a grooved anode," *Chemical Engineering Research and Design*, 79 (4) (2001), 383-388.
10. A. Caboussat et al., "Large Gas Bubbles under the Anodes of Aluminum Electrolysis Cells", *Light Metals*, (2011), 581-586.
11. J.R. Grace et al., "Shapes and velocities of single drops and bubbles moving freely through immiscible liquids," *Trans. Inst. Chem. Eng*, 54 (3) (1976), 167-173.
12. D. Bhaga and M.E. Weber, "Bubbles in viscous liquids: shapes, wakes and velocities," *Journal of Fluid Mechanics*, 105 (1981), 61-85.
13. K. Qian et al., "Visual observation of bubbles at horizontal electrodes and resistance measurements on vertical electrodes," *Journal of Applied Electrochemistry*, 27 (4) (1997), 434-440.
14. K. Qian et al., "Bubble coverage and bubble resistance using cells with horizontal electrode," *Journal of Applied Electrochemistry*, 28 (10) (1998), 1141-1145.
15. M. Alam et al., "Investigation of Anodic Gas Film Behavior in Hall–Heroult Cell Using Low Temperature Electrolyte," *Metallurgical and Materials Transactions B*, 44 (5) (2013), 1155-1165.
16. M.C. Ruzicka, "On dimensionless numbers," *Chemical Engineering Research and Design*, 86 (8) (2008), 835-868.
17. X. Miao, D. Lucas, Z. Ren, S. Eckert and G. Gerbeth, "Numerical modeling of bubble-driven liquid metal flows with external static magnetic field," *International Journal of Multiphase Flow*, 48 (2013), 32-45.
18. S. Das et al., "Theoretical Investigation of the Inclined Sidewall Design on Magnetohydrodynamic (MHD) Forces in an Aluminum Electrolytic Cell," *Metallurgical and Materials Transactions B*, 42 (1) (2011), 243-253.
19. S. Das, Y.S. Morsi, G. Brooks, J.J.J Chen and W. Yang, "Principal characteristics of a bubble formation on a horizontal downward facing surface," *Colloids and Surfaces A: Physicochemical and Engineering Aspects*, 411 (2012), 94-104.